

# Redefining the tail of pancreas based on the islets microarchitecture and inter-islet distance

## An immunohistochemical study

Praveen Kumar Ravi, MD<sup>a</sup>, Sudipta Ranjan Singh, MD<sup>b</sup>, Pravash Ranjan Mishra, MD, DMRD<sup>c,\*</sup>

### Abstract

Researchers divided the pancreas distal to the neck into 2 equal parts as the body and tail region by an arbitrary line. Surgeons considered the part of the pancreas, left to the aorta as the tail region. We performed this study to identify the transition zone of low-density to high-density islet cells for redefining the tail region.

We quantified islets area proportion, beta-cell area proportion, and inter-islet distance in 9 Indian-adult-human non-diabetic pancreases from autopsy by using anti-synaptophysin and anti-insulin antibodies. Data were categorized under 3 regions like the proximal body, distal body, and distal part of the pancreas.

Islet and beta-cell area proportion are progressively increased from head to tail region of the pancreas with a significant reduction in inter-islet distance and beta-cell percentage distal to the aorta. There is no significant difference in inter-islet distance and beta-cell percentage of the distal part of the body and tail region.

Crowding of islets with intermingled microarchitecture begins in the pancreas distal to the aorta, which may be the beginning of the actual tail region. This study will provide insight into the preservation of islets-rich part of the pancreas during pancreatectomy and future prediction of new-onset diabetes.

**Abbreviations:** AJCC = American Joint Committee on Cancer, B1 = part of body right to the aorta, B2 = part of body left to the aorta, DAB = 3,3'-diaminobenzidine, H = head, HRP = horseradish peroxidase, IHC = immunohistochemistry, IID = inter-islet distance, NODM = new-onset diabetes, T = tail, WSI = whole slide image.

**Keywords:** inter-islet distance, islets, pancreatic resection

## 1. Introduction

The pancreas has a unique scattered distribution of islets, which not only vary in their microarchitecture but also in its proportion to the exocrine part in various regions of the pancreas. Recent studies

documented the intra-pancreatic regional variability of islets area proportion.<sup>[1]</sup> Islets of different parts of the pancreas are varying in their embryogenesis, architecture, and insulin secretory capacity.<sup>[2-4]</sup> Islets in the tail region are derived from the dorsal pancreatic bud and these islets are relatively larger in size with the characteristic intermingling of relatively fewer beta cells with more alpha cells, which increase their insulin-secreting capacity via paracrine effect.<sup>[5,6]</sup> Since the islet distribution/density is relatively higher (twice that of the head) in the tail region,<sup>[7]</sup> obviously, the inter-islet distance (IID) will be less due to overcrowding of islets.

Even though many studies emphasizing on the importance of the pancreatic islets on the tail region, there is paucity on the studies which actually delineate the tail region.<sup>[8]</sup> The classical anatomy textbook describes the tail region as part of the pancreas within the layers of the splenorenal ligament.<sup>[9]</sup> Most of the pancreas researchers for the purpose of histomorphometric studies considered tail and body as 2 equal parts.<sup>[10]</sup> As per the American Joint Committee on Cancer (AJCC) guidelines, surgeons considering the part of the pancreas left to the aorta as the tail region.<sup>[11]</sup> Despite the importance of the islets of tail region in comparison with islets of other parts of the pancreas, there is a paucity of literature that exactly demarcates the tail region where the islets density is relatively higher than the rest of the pancreas. Detailed knowledge about the beginning of the tail region where the islet density starts rising is essential to preserve islet rich part during pancreatic surgeries, to predict the future risk of new-onset diabetes (NODM) following pancreatectomy and to improve the islet harvesting.

Furthermore, the quantification of exact islet area proportion or individual islet cell composition in different regions of the

Editor: Xiaodun Yang.

The research was supported by Thesis Grant (No. 3/2/June-2017/PG-Thesis-HRD [14]) of the Indian Council of Medical Research, New Delhi, India.

The authors declare that the research was conducted in the absence of any conflict of interest.

The datasets generated during and/or analyzed during the current study are available from the corresponding author on reasonable request.

<sup>a</sup> Department of Anatomy, Trichy SRM Medical College Hospital & Research Centre, Tiruchirappalli, Tamil Nadu, 621105, India., <sup>b</sup> Department of Forensic Medicine and Toxicology, <sup>c</sup> Department of Anatomy, All India Institute of Medical Sciences, Bhubaneswar, Odisha, India.

\* Correspondence: Pravash Ranjan Mishra, Room No. 1, Department of Anatomy, Academic Block, All India Institute of Medical Sciences, Bhubaneswar, Odisha, 751019, India (e-mail: mishra.pravash@yahoo.com).

Copyright © 2021 the Author(s). Published by Wolters Kluwer Health, Inc. This is an open access article distributed under the terms of the Creative Commons Attribution-Non Commercial License 4.0 (CCBY-NC), where it is permissible to download, share, remix, transform, and buildup the work provided it is properly cited. The work cannot be used commercially without permission from the journal.

How to cite this article: Ravi PK, Singh SR, Mishra PR. Redefining the tail of pancreas based on the islets microarchitecture and inter-islet distance: an immunohistochemical study. *Medicine* 2021;100:17(e25642).

Received: 16 November 2020 / Received in final form: 17 March 2021 /

Accepted: 20 March 2021

<http://dx.doi.org/10.1097/MD.00000000000025642>

human pancreas is challenging due to its complex distribution. The majority of the existing studies have quantified the endocrine part by taking a limited number of tissue sections, restricted to certain regions of the pancreas or by selecting the pancreatic tissue blocks randomly.<sup>[12–14]</sup> The pancreatic islets are known for high regional variability, so this random or restricted selection of tissue will result in under or overestimation of islets area.<sup>[15]</sup> Furthermore, few studies have selected random microscopic fields or islet-rich fields for measuring the proportion of endocrine part leading to selection bias.<sup>[1]</sup>

So, the present study aimed to determine the location of transition zone in the pancreas, that is, the beginning of the actual tail region of the human pancreas where the islet density is start rising or differ significantly based on the inter-islet distance and endocrine area proportion (beta-cell percentage) by using large-scale computer-assisted analysis.

## 2. Materials and methods

### 2.1. Pancreas collection

A total of 9 adult human pancreases were collected from autopsy within 12 hours of death after obtaining the institutional ethical committee approval.<sup>[16]</sup> In all the cases, the cause of death was the road traffic accident; none of the cases were suffering from any chronic disorders like diabetes, pancreatitis, etc. The pancreas was divided into anatomical head, body, and tail based on the previous studies<sup>[10,17]</sup> (Fig. 1). Briefly, after removing the head (H) by dividing at the neck (using portal vein as a landmark), part of the pancreas distal to the portal vein is divided into 2 equal parts as the anatomical body and tail region (T) (Fig. 1). Secondly, based on AJCC surgical guidelines,<sup>[11]</sup> the body is subdivided into 2 parts (part of body right to the aorta [B1] and part of body left to the aorta [B2]) by using the left margin of the aorta as the landmark. All 4 segments were labeled, as shown in Figure 1. Subsequently, complete coronal and transverse sections of all the 4 parts of the pancreas were grossed as described earlier.<sup>[17]</sup> Approximately 40 sub-blocks from each pancreas were immersion fixed in 10% neutral buffered formalin, processed, and embedded in paraffin blocks. Pancreas showing

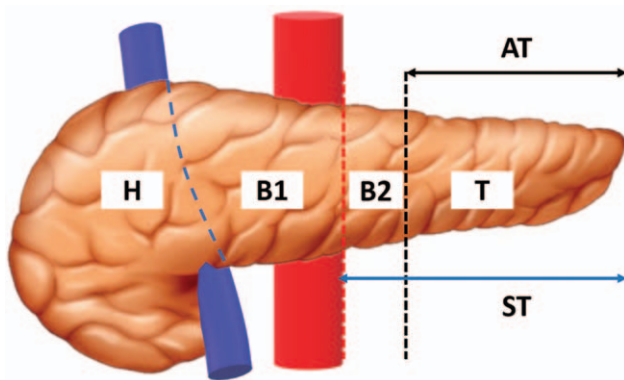


**Figure 1.** Pancreatic head (H) is divided by using portal vein as a landmark (blue dotted line); body and tail region (T) of the pancreas is divided into 2 equal halves (black dotted line); the body of the pancreas is subdivided as B1 (part of body right to the aorta) (red dotted line) and B2 (part of the body left to the aorta) based on AJCC guidelines. AJCC=American Joint Committee on Cancer; AT=anatomical tail (T); ST=surgical tail (B2+T).

autolytic changes and occult pancreatitis in Hematoxylin and Eosin staining were excluded from the study.

### 2.2. Immunohistochemistry

Immunohistochemistry (IHC) was done on 2 consecutive 4  $\mu\text{m}$  thick paraffin sections from each block. Antigen retrieval was done by using the heat antigen retrieval method under high pressure with a citrate buffer solution. After blocking the endogenous peroxidase activity, primary antibodies such as rabbit monoclonal anti-synaptophysin antibody (1:300) (PathnSitu, Livermore, California) and rabbit monoclonal anti-insulin antibody (1:200) (PathnSitu, Livermore, California) were used. The primary antibody was detected by a secondary antibody labeled with horseradish peroxidase (HRP) and 3,3'-diaminobenzidine (DAB) chromogen (DAKO, Carpinteria, CA). Whole slide images of all IHC slides were captured in 10 $\times$  magnification by using Carl Zeiss digital slide scanning system and Meta-Systems software. 10 $\times$  magnification was sufficient for computer-assisted image analysis.<sup>[18]</sup> Each whole slide image (WSI) sized several gigabytes were exported into the TIFF format and were transported to the workstation.

### 2.3. Quantification

All WSIs were analyzed by using Fiji/ImageJ free software from NIH (downloaded from <http://imagej.nih.gov/>). We quantified the islets and beta-cell area proportion as per our previous publication.<sup>[17]</sup> In addition to that, following the segmentation of synaptophysin stained WSIs, the inter islet distance of each islet was measured by using the nearest neighbor distances plugin in ImageJ software<sup>[19]</sup> (Fig. 2B and C). The IID was measured from the center of each islet to the center of nearby islets. The islet area less than 17  $\mu\text{m}^2$  was excluded as these are scattered islets cells rather than individual islets.

The formula used for various calculations are:

1. Islet area proportion = [total DAB positive area of the slide (anti-synaptophysin)]/[total tissue area of the slide]  $\times$  100.
2. Beta-cell area proportion = [total DAB positive area of the slide (anti-insulin)]/[total tissue area of the slide]  $\times$  100.
3. Beta-cell percentage = [total beta-cell area]/[total islet area]  $\times$  100.

Here the authors calculated the beta-cell percentage against the total islet area in different parts of the pancreas.

### 2.4. Statistical analysis

Data are summarized and expressed as mean  $\pm$  SD. Paired “*t*” test was used to compare the data of means of the islet and beta-cell area proportion, beta-cell percentage, and IID in various regions of the pancreas. Pearson correlation test was used to compare the relation of islet areas proportion and inter-islet distance. *P* value  $<$ .05 taken as significant. The statistical test was performed by using SPSS software version 25 and graphs were plotted by Microsoft Excel 2016 software.

## 3. Results

Details of the 9 subjects, including age, gender, and BMI were given in Table 1. In all cases, BMI is within a reasonable limit.

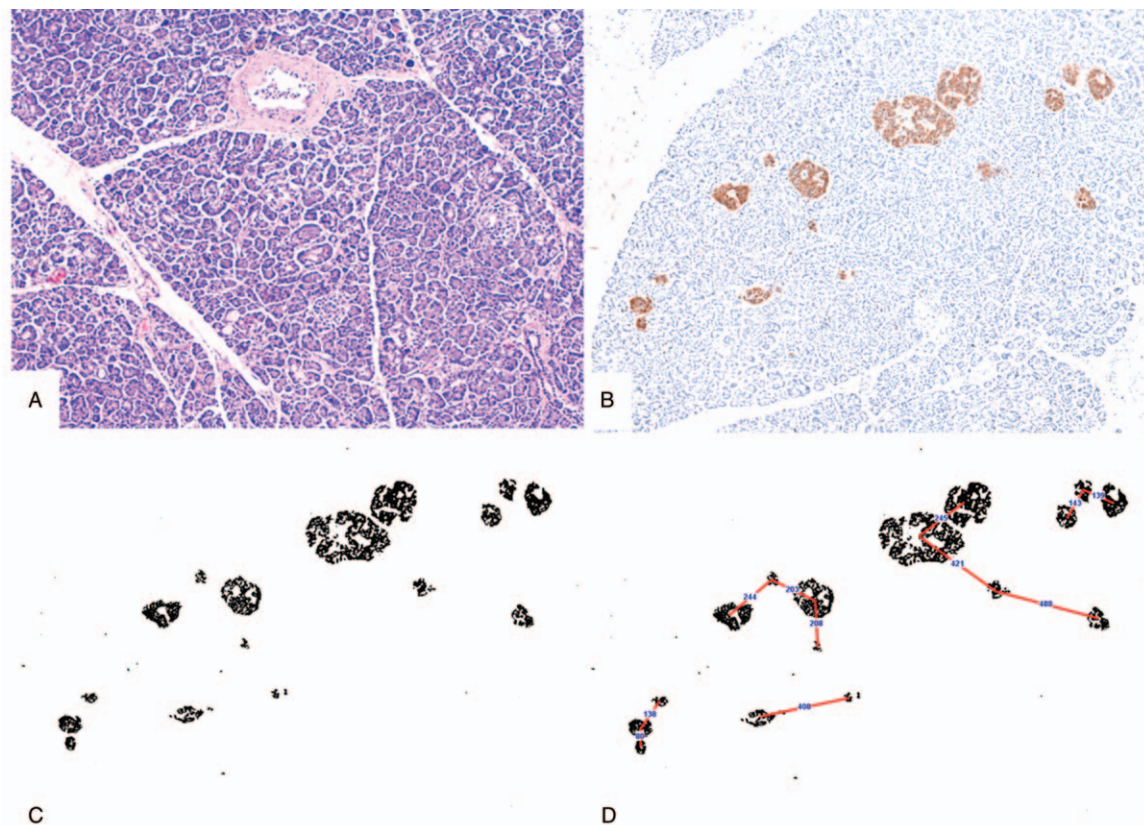


**Figure 2.** (A) Hematoxylin and Eosin-stained section showing pancreatic islets and acini without features of autolysis; (B) a single representative field of IHC image, stained by an anti-synaptophysin antibody from B1 segment of a pancreas; (C) processed image – segmentation of DAB positive area in ImageJ software; (D) schematic representation showing how the ImageJ software calculated the IID – centre of each islet to the centre of the nearby islet. Images B, C, and D are at same magnification for better comparison. IHC=immunohistochemistry, IID=inter-islet distance

**3.1. Topographical variation of islets and beta-cell area proportion**

Topographical variation of islet and beta-cell area proportion of all the 9 cases were plotted in the bar graph with its corresponding inter-islets distances in Figure 3. The mean islet area proportion of B1, B2, and T segment was  $0.75 \pm 0.29\%$ ,  $0.99 \pm 0.34\%$ , and  $1.37 \pm 0.65\%$  respectively. The mean beta-cell area proportion of B1, B2, and T segment was  $0.58 \pm 0.26\%$ ,  $0.7 \pm 0.31\%$ , and  $0.93 \pm 0.43\%$ , respectively. The mean islets and beta-cell area proportions are progressively increasing from the

body to the tail region of the pancreas (Table 2). Islets and beta-cell area proportion of B2 segment (part of the body left to the aorta) is significantly higher than that of B1 segment with the *P* value of .007 and .021, respectively. Thus, there is a significant rise in endocrine proportion in the distal part of the body (B2 segment).

**3.2. Topographical variation of islet dimension**

The mean islet dimensions of B1, B2, and T segment of the pancreas are  $42.34 \pm 5.19 \mu\text{m}$ ,  $43.62 \pm 8.24 \mu\text{m}$ , and  $45.62 \pm 4.67 \mu\text{m}$ , respectively. The mean islet dimension increased from the B1 to T segment; however, there is no significant difference (*P* value = .3).

**3.3. Topographical variation of inter-islet distances**

The mean inter-islet distances of B1, B2, and T segment of the pancreas are  $268.1 \pm 62.3 \mu\text{m}$ ,  $232.6 \pm 49.9 \mu\text{m}$ , and  $210.54 \pm 39.7 \mu\text{m}$ , respectively. The mean inter-islet distance was progressively decreasing from body to tail region of the pancreas. The mean inter-islet distance of the B2 segment is significantly lower than that of the B1 segment; however, there is no significant difference between the IID of the B2 and T segment. Thus, crowding of islets starts in the distal part of the anatomical body. There is a strong negative correlation of IID and islet area

**Table 1**  
Details of the subjects.

| Case No. | Age | Gender | BMI      |
|----------|-----|--------|----------|
| 1        | 45  | F      | 21.31659 |
| 2        | 34  | F      | 18.91807 |
| 3        | 35  | F      | 20.3428  |
| 4        | 49  | M      | 18.02289 |
| 5        | 30  | F      | 20.56881 |
| 6        | 34  | F      | 20.88889 |
| 7        | 75  | M      | 18.32963 |
| 8        | 27  | M      | 19.77041 |
| 9        | 25  | M      | 28.47898 |

BMI=body mass index.

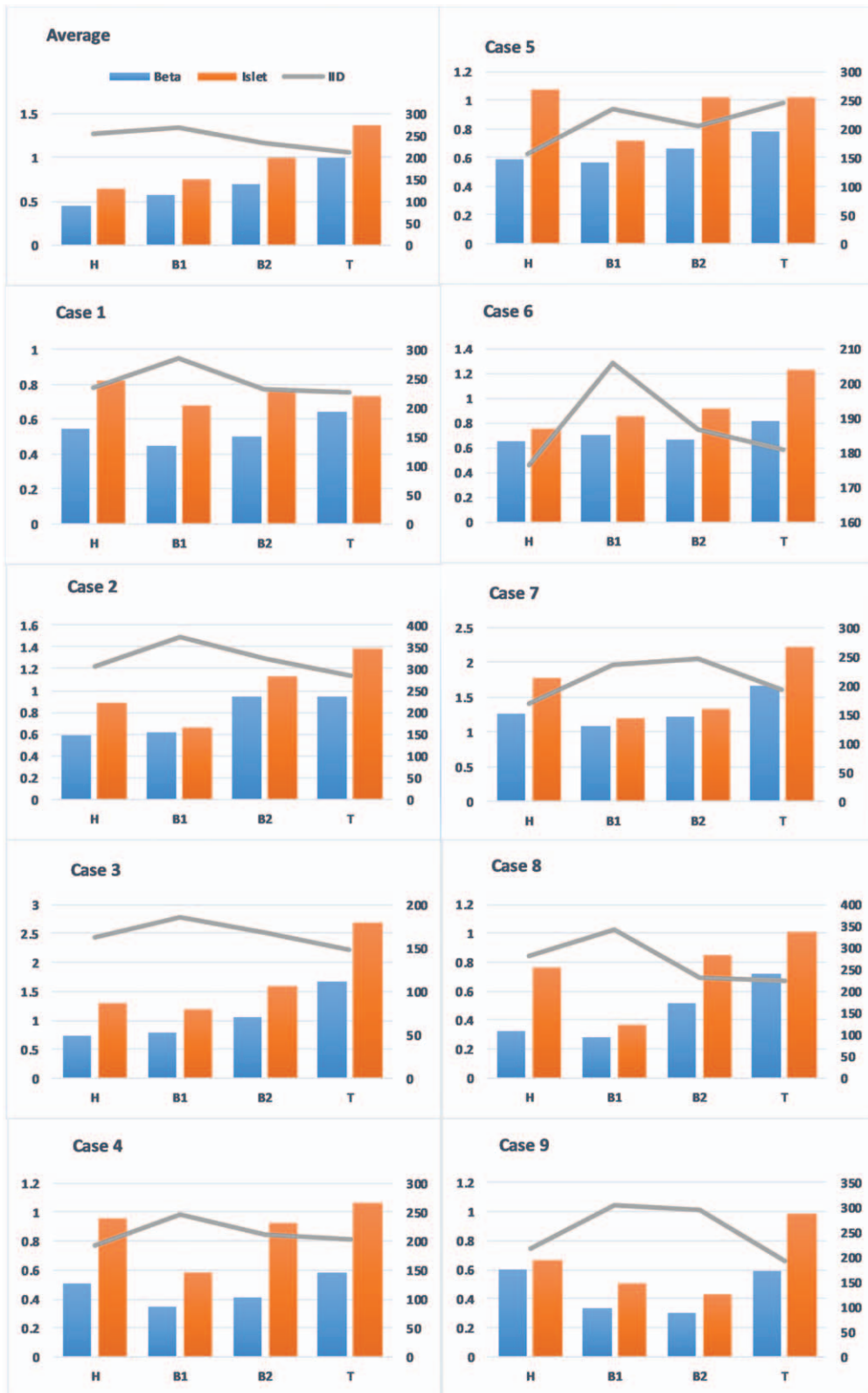


**Figure 3.** Bar chart representing the topographical variation of islets and beta-cell area proportion with its corresponding IID of all the 9 cases along with its mean values (average). IID was reduced in the B2 segment in most of the cases, which is almost similar to that of the T segment. Case nos. 5 and 7 show the difference in IID trend when compared with the general trend; out of that 2 cases, case no. 7 is the 70yr old male; thus, the cases might be because of age-related changes in the pancreas. IID=inter-islet distance.

**Table 2**

**Regional variation of islet and beta-cell area proportion, inter-islet distance, and beta-cell percentage to total islet area.**

|    | Islet area proportion |                  | Beta-cell area proportion |                  |
|----|-----------------------|------------------|---------------------------|------------------|
|    | Mean ± SEM            | P                | Mean ± SEM                | P                |
| B  | 0.87 ± 0.30%          | B vs T = .005*   | 0.62 ± 0.28%              | B vs T = .001*   |
| B1 | 0.75 ± 0.29%          | B1 vs B2 = .007* | 0.58 ± 0.26%              | B1 vs B2 = .021* |
| B2 | 0.99 ± 0.34%          | B2 vs T = .021*  | 0.7 ± 0.31%               | B2 vs T = .006*  |
| T  | 1.37 ± 0.65%          |                  | 0.93 ± 0.43%              |                  |

|    | Inter-islet distance |                  | Beta-cell percentage to total islet area |                  |
|----|----------------------|------------------|--|------------------|
|    | Mean ± SEM           | P                | Mean ± SEM                               | P                |
| B  | 250.1 ± 56.1 μm      | B vs T = .013*   | 70.1 ± 13.8%                             | B vs T = .844    |
| B1 | 268.1 ± 62.3 μm      | B1 vs B2 = .016* | 75.7 ± 12.2%                             | B1 vs B2 = .036* |
| B2 | 232.6 ± 49.9 μm      | B2 vs T = .130   | 69.1 ± 13.3%                             | B2 vs T = .986   |
| T  | 210.54 ± 39.7 μm     |                  | 69.2 ± 9.9%                              |                  |

B=anatomical body, B1=part of body right to the aorta, B2=part of the body left to the aorta, T=anatomical tail.

proportion, confirmed with Pearson correlation and had  $r = -0.579$ ,  $P < .002$ ; which is statistically significant (Fig. 4).

**3.4. Topographical variation of beta-cell area percentage to total islet area**

The mean beta-cell area percentage of B1, B2, and T segment was  $75.7 \pm 12.2\%$ ,  $69.1 \pm 13.3\%$ , and  $69.2 \pm 9.9\%$ , respectively. The mean beta-cell area percentage of the B2 segment is significantly lower than that of the B1 segment; however, there is no significant difference between the mean beta-cell area percentage of the B2 and T segment.

**4. Discussion**

The pancreas is an exo-endocrine organ that regulates body metabolism. Endocrine cells are scattered within the exocrine

pancreas, which constitutes around 2% of the total pancreatic area. In standard textbooks, there is no clear demarcation of the tail region from the body. The proportion of islets and beta cells are higher in the distal part of the pancreas. This differential distribution may be due to the variable sources of its embryological origin.<sup>[1,7,20]</sup> Even though the size of the pancreas varies widely from rodents to monkeys or humans, the size of the islet is almost remaining constant, with the maximum diameter being around 500 μm.<sup>[6,7]</sup> Thus, several researchers hypothesized that the optimal size of the islet is essential for its adequate functional activity.<sup>[2,4,21]</sup> To meet the insulin demand, the islet number (limiting islet size) and its cellular arrangement are increased during evolution.<sup>[6]</sup> This intermingled arrangement of alpha and beta cells allows the contact of single beta cells with more number of alpha cells, which increase the insulin-secreting capacity of beta cells via the paracrine effect.<sup>[6]</sup>

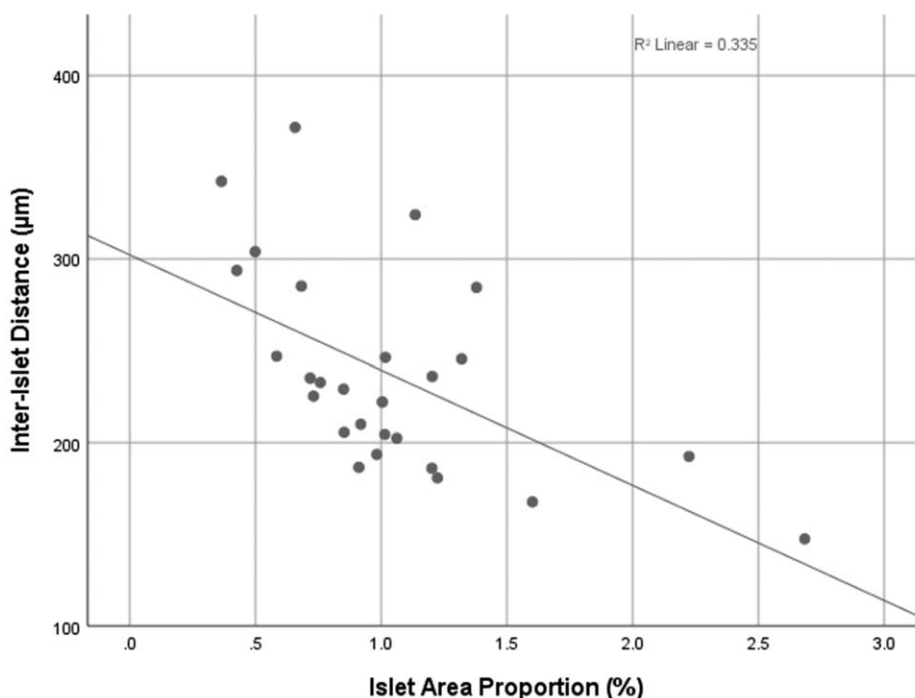


**Figure 4.** Relation of islet area proportion and inter-islet distance.

Topographical variation of islets morphology and functions is also linked with their development.<sup>[2–4]</sup> Islets derived from the dorsal pancreatic bud (distal part of the pancreas) are relatively larger in size with the characteristic intermingled arrangement of alpha and beta cells, which has higher insulin-secreting capacity than that of islet-derived from the ventral bud (lower part of the head).<sup>[4,7]</sup> Some animal studies demonstrated that the basal insulin-secreting capacity of islets derived from both ventral and dorsal buds is similar; however, the insulin-secreting capacity of islet-derived from the dorsal pancreatic bud is significantly higher even in the lower glucose concentration via the paracrine effect.<sup>[2–4]</sup>

Topographical variation in islet distribution, like more than two-fold (100%) increase in islet area proportion in the distal part<sup>[7]</sup> is probably due to an increase in islets number rather than size.<sup>[6]</sup> The present study also documented no significant variation in islet dimension in the body and tail region of the pancreas. The increase in islet number leads to crowding of the islets, which results in the reduction of the IID. Though the larger islets with characteristic intermingling arrangement of alpha and beta cells are more efficient in insulin secretion, there is a reduction in beta-cell area percentage to total islets area.<sup>[17]</sup> Thus, in the present study, we used the IID and beta-cell area percentages to determine the tail region.

In the present study, the authors observed a reduction in IID in the part of the pancreas left to the aorta (B2 and T segment) (Table 2). Even though both islet and beta-cell area proportion increase from the body to tail, it is increasing disproportionately. Islet area proportion increases 24% from B1 to B2 region, whereas beta-cell area proportion increases 12% only (Table 2). Thus, there is a reduction in beta-cell percentage to total islet area in the B2 region. Increasing in islet areas with a significant reduction in the beta-cell percentage in the B2 region shows the appearance of larger islets with characteristic intermingled alpha and beta cells, as seen in similar studies.<sup>[6,17]</sup> In the region left to the aorta (B2 and T region), both islet and beta-cell area proportion increased ~40% symmetrically (Table 2) leading to no differences in the beta-cell percentage to total islet area, which shows there is no change in islet architecture (size and cellular arrangement) in both these areas. Even though there is a significant increase in islet and beta-cell area proportion between B2 and T segments, the B2 segment shows the characteristic islet crowding and intermingled beta and alpha cells arrangement as observed in the T region. Thus, the B2 and T segment has histomorphometric similarities in islets distribution and architecture. The entire part of the pancreas left to the aorta may be considered as the tail of the pancreas.

Distal or left pancreatectomy may range from resection of the smaller region of the tail to complete resection body and tail region, which is commonly done in the cancerous or premalignant lesions of the pancreas. Approximately 70% of islets are lost during total resection of the pancreas distal to the neck (extended left pancreatectomy). Thus, NODM (type 3c diabetes mellitus)<sup>[22]</sup> is commonly encountered in 5% to 50% of the individuals based on the extent of the pancreatic resection and pre-existing disease status of the individual.<sup>[23,24]</sup> The incidence of NODM is higher in the distal pancreatectomy individuals when compared with the other type of pancreatectomies (Table 3).<sup>[23,25–34]</sup> Apart from endocrine insufficiency, exocrine insufficiency is also reported in 20.19% of distal pancreatectomy individuals.<sup>[33]</sup> So optimal resection is essential to avoid metabolic derangement and subsequent morbidities.

**Table 3**

**Review of literature shows the incidence of new-onset diabetes mellitus (NODM) in the distal pancreatectomy (DP).**

| S. No. | Author (year)              | NODM in DP (%) |
|--------|----------------------------|----------------|
| 1      | Schnelldorfer et al (2007) | 51             |
| 2      | King et al (2008)          | 20–50          |
| 3      | Kim et al (2011)           | 19.2           |
| 4      | Burkhardt et al (2015)     | 31             |
| 5      | De Bruijin et al (2015)    | 17–36          |
| 6      | Kwon et al (2015)          | 30.5           |
| 7      | Kang et al (2016)          | 25.3           |
| 8      | Nguyen et al (2017)        | 44.6           |
| 9      | Woodcock et al (2019)      | 4–5            |
| 10     | Jiro et al (2019)          | 44.79          |
| 11     | Wu et al (2020)            | 3–40           |

As the pancreas shows a high degree of intra-pancreatic regional variability in islets morphology and distribution, we quantified the islet and beta-cell areas proportion by examining the WSI of a complete representative coronal and sagittal section of the pancreas tissue (at least 20 cm<sup>2</sup> area microscopically in each pancreas) using large-scale computer-assisted analysis with Image J software. This method of analysis minimizes the sampling error and interobserver variation. Furthermore, researchers in various studies have determined the total islet area proportion by adding 3 major endocrine cells of islets like alpha-, beta-, and delta cells, which leads to an underestimation of total islets area due to ignoring the minor endocrine cells like epsilon and pancreatic polypeptide cells.<sup>[1,15,20]</sup> The anti-synaptophysin antibody used in the present study is against the transmembrane vesicle protein of islets cell, which shows immunoreactivity toward all subtypes of islets cells resulting in less chance of underestimation of islet area.<sup>[35]</sup>

The limitation of the present study is that even though we have collected the pancreas from individuals without a history of diabetes, there may be chances of subclinical diabetes. We have examined the reports of recent blood sugar values wherever available to exclude the diabetic pancreases. The other limitation of the present study is case no 7 (Table 1 and Fig. 3), which is the pancreas of a 75-years old male, who is a relatively older individuals in the study. The IID and beta-cell percentages show no significant change in B1 and B2 segment; this might be due to age-related changes in the pancreas.<sup>[36,37]</sup>

In conclusion, for the first time, we provided information about the beginning of the tail of the pancreas based on the histomorphometric features by using large-scale computer-assisted analysis. Part of the pancreas distal to the aorta contains a higher density of relatively larger islet with more insulin-secreting capacity. Even though the amount of the pancreatic resection in distal pancreatectomy is decided based on the extent and nature of the disease, knowledge about the topographical variation of islet density in the pancreas will provide an insight into the better preservation of islets during pancreatic surgery and prediction of future risk of diabetes and other comorbid conditions.

### Acknowledgments

Preliminary results of the study were presented in the European Pancreatic Club virtual meeting 2020.

## Author contributions

**Conceptualization:** Praveen Kumar Ravi, Pravash Ranjan Mishra.

**Data curation:** Praveen Kumar Ravi, Sudipta Ranjan Singh.

**Formal analysis:** Praveen Kumar Ravi, Pravash Ranjan Mishra.

**Funding acquisition:** Praveen Kumar Ravi, Pravash Ranjan Mishra.

**Investigation:** Praveen Kumar Ravi.

**Methodology:** Praveen Kumar Ravi, Sudipta Ranjan Singh, Pravash Ranjan Mishra.

**Project administration:** Pravash Ranjan Mishra.

**Resources:** Pravash Ranjan Mishra.

**Software:** Praveen Kumar Ravi.

**Supervision:** Pravash Ranjan Mishra.

**Validation:** Praveen Kumar Ravi, Pravash Ranjan Mishra.

**Visualization:** Pravash Ranjan Mishra.

**Writing – original draft:** Praveen Kumar Ravi.

**Writing – review & editing:** Sudipta Ranjan Singh, Pravash Ranjan Mishra.

## References

- [1] Olehnik SK, Fowler JL, Avramovich G, et al. Quantitative analysis of intra-and inter-individual variability of human beta-cell mass. *Sci Rep* 2017;7:1–7.
- [2] Trimble ER, Renold AE. Ventral and dorsal areas of rat pancreas: islet hormone content and secretion. *Am J Physiol Metab* 2017;240:E422–7.
- [3] Leclercq-Meyer V, Marchand J, Malaisse WJ. Insulin and glucagon release from the ventral and dorsal parts of the perfused pancreas of the rat. *Horm Res* 1985;21:19–32.
- [4] Trimble ER, Halban PA, Wollheim CB, et al. Functional differences between rat islets of ventral and dorsal pancreatic origin. *J Clin Invest* 1982;69:405–13.
- [5] Kilimnik G, Zhao B, Jo J, et al. Altered islet composition and disproportionate loss of large islets in patients with type 2 diabetes. *PLoS One* 2011;6:e27445.
- [6] Kim A, Miller K, Jo J, et al. Islet architecture: a comparative study. *Islets* 2009;1:129–36.
- [7] Wang X, Misawa R, Zielinski MC, et al. Regional differences in islet distribution in the human pancreas – preferential beta-cell loss in the head region in patients with type 2 diabetes. *PLoS One* 2013;8:1–9.
- [8] Desouza SV, Yoon HD, Singh RG, et al. Quantitative determination of pancreas size using anatomical landmarks and its clinical relevance: a systematic literature review. *Clin Anat* 2018;31:913–26.
- [9] Standring S. *Gray's Anatomy: The Anatomical Basis of Clinical Practice*. 41st ed New York: Elsevier Churchill Livingstone; 2016.
- [10] Campbell-Thompson ML, Montgomery EL, Foss RM, et al. Collection protocol for human pancreas. *J Vis Exp* 2012;63:1–5.
- [11] Amin MB, Edge SB, Greene FL, et al. *AJCC Cancer Staging Manual*. Cham: Springer International Publishing; 2017.
- [12] Ionescu-Tirgoviste C, Gagniuc PA, Gubceac E, et al. A 3D map of the islet routes throughout the healthy human pancreas. *Sci Rep* 2015;5:1–14.
- [13] Saisho Y, Butler AE, Manesso E, et al.  $\beta$ -Cell mass and turnover in humans: effects of obesity and aging. *Diabetes Care* 2013;36:111–7.
- [14] Jones LC, Clark A. B-Cell neogenesis in type 2 diabetes. *Diabetes* 2001;50:14–5.
- [15] Poudel A, Fowler JL, Zielinski MC, et al. Stereological analyses of the whole human pancreas. *Sci Rep* 2016;6:1–13.
- [16] Ravi PK, Purkait S, Singh SR, et al. Decay score: a guide to the immunoreactivity of human pancreatic islets in autopsy specimen. *Folia Morphol (Warsz)* 2021;published online.
- [17] Ravi PK, Purkait S, Agrawal U, et al. Regional variation of human pancreatic islets dimension and its impact on beta cells in Indian population. *Islets* 2019;11:141–51.
- [18] Kilimnik G, Jo J, Periwal V, et al. Quantification of islet size and architecture. *Islets* 2012;4:167–72.
- [19] Mao Y. Nearest Neighbor Distances Calculation with ImageJ. [https://icme.hpc.msstate.edu/mediawiki/index.php/Nearest\\_Neighbor\\_Distances\\_Calculation\\_with\\_ImageJ](https://icme.hpc.msstate.edu/mediawiki/index.php/Nearest_Neighbor_Distances_Calculation_with_ImageJ). Published 2016. Accessed March 27, 2020.
- [20] Wang X, Zielinski MC, Misawa R, et al. Quantitative analysis of pancreatic polypeptide cell distribution in the human pancreas. *PLoS One* 2013;8:1–7.
- [21] Gittes GK. Developmental biology of the pancreas: a comprehensive review. *Dev Biol* 2009;326:4–35.
- [22] Maxwell DW, Jajja MR, Galindo RJ, et al. Post-pancreatectomy diabetes index: a validated score predicting diabetes development after major pancreatectomy. *J Am Coll Surg* 2020;230:393–402.e3.
- [23] De Buijn KMJ, Van Eijck CHJ. New-onset diabetes after distal pancreatectomy: a systematic review. *Ann Surg* 2015;261:854–61.
- [24] Maxwell DW, Jajja MR, Tariq M, et al. Development of diabetes after pancreaticoduodenectomy: results of a 10-year series using prospective endocrine evaluation. *J Am Coll Surg* 2019;228:400–12.e2.
- [25] Schnelldorfer T, Lewin DN, Adams DB. Operative management of chronic pancreatitis: longterm results in 372 patients. *J Am Coll Surg* 2007;204:1039–45.
- [26] King J, Kazanjian K, Matsumoto J, et al. Distal pancreatectomy: incidence of postoperative diabetes. *J Gastrointest Surg* 2008;12:1548–53.
- [27] Kim K-J, Jeong C-Y, Jeong S-H, et al. Pancreatic diabetes after distal pancreatectomy: incidence rate and risk factors. *Korean J Hepato-Biliary-Pancreatic Surg* 2011;15:123.
- [28] Burkhart RA, Gerber SM, Tholey RM, et al. Incidence and severity of pancreatogenic diabetes after pancreatic resection. *J Gastrointest Surg* 2015;19:217–25.
- [29] Kwon JH, Kim SC, Shim IK, et al. Factors affecting the development of diabetes mellitus after pancreatic resection. *Pancreas* 2015;44:1296–303.
- [30] Kang JS, Jang JY, Kang MJ, et al. Endocrine function impairment after distal pancreatectomy: incidence and related factors. *World J Surg* 2016;40:440–6.
- [31] Nguyen A, Demirjian A, Yamamoto M, et al. Development of postoperative diabetes mellitus in patients undergoing distal pancreatectomy versus whipple procedure. *Am Surg* 2017;83:1050–3.
- [32] Woodcock L. Diabetes care after pancreatic surgery. *J Diabetes Nurs* 2019;23:1–5.
- [33] Kusakabe J, Anderson B, Liu J, et al. Long-term endocrine and exocrine insufficiency after pancreatectomy. *J Gastrointest Surg* 2019;23:1604–13.
- [34] Wu L, Nahm CB, Jamieson NB, et al. Risk factors for development of diabetes mellitus (Type 3c) after partial pancreatectomy: a systematic review. *Clin Endocrinol (Oxf)* 2020;92:396–406.
- [35] Redecker P, Jörns A, Jahn R, et al. Synaptophysin immunoreactivity in the mammalian endocrine pancreas. *Cell Tissue Res* 1991;264:461–7.
- [36] Mizukami H, Takahashi K, Inaba W, et al. Age-associated changes of islet endocrine cells and the effects of body mass index in Japanese. *J Diabetes Investig* 2014;5:38–47.
- [37] Yagihashi S, Inaba W, Mizukami H. Dynamic pathology of islet endocrine cells in type 2 diabetes:  $\beta$ -cell growth, death, regeneration and their clinical implications. *J Diabetes Investig* 2016;7:155–65.